Jpn J Radiol (2010) 28:299–304
DOI 10.1007/s11604-010-0427-z

ORIGINAL ARTICLE

Precontrast and postcontrast susceptibility-weighted imaging in the assessment of intracranial brain neoplasms at 1.5 T

**Masaaki Hori · Keiichi Ishigame · Hiroyuki Kabasawa
Hiroshi Kumagai · Satoshi Ikenaga · Nobuyuki Shiraga
Shigeki Aoki · Tsutomu Araki**

Received: August 24, 2009 / Accepted: February 4, 2010

Abstract
Purpose. The goal of this study was to estimate pre- and post-gadolinium-enhanced high-spatial resolution susceptibility-weighted imaging (SWI) in patients with brain neoplasms.
Materials and methods. A total of 17 patients (8 women, 9 men) with brain neoplasms participated in this study. In addition to conventional magnetic resonance imaging, pre- and post-gadolinium-enhanced SWI was performed. The contrast-to-noise ratio (CNR) and major diameters of the brain tumor were measured for quantitative analyses, and intratumoral susceptibility signal intensity (ITSS) was graded for semiquantitative analysis.
Results. Both bright and dark enhancement were observed at the pathological lesion on postcontrast SWI. Some postcontrast SWI results suggested leakage of contrast material due to breakdown of the blood-brain barrier. There were no statistical differences (Student's *t*-test) between postcontrast SWI and three-dimensional (3D) T1-weighted images regarding the major diameters of the brain tumors. CNR of postcontrast 3D T1-weighted images was statistically superior to that of postcontrast SW images ($P < 0.01$, Wilcoxon signed-rank test). Malignant tumors tended to have a higher ITSS score.
Conclusion. SWI clearly visualized the architecture of brain neoplasms. This imaging technique may be useful for evaluating tumor characterization in clinical use.

Key words MRI · Susceptibility-weighted imaging · Contrast enhancement · Brain neoplasm

M. Hori (✉) · K. Ishigame · H. Kumagai · S. Ikenaga · T. Araki
Department of Radiology, University of Yamanashi, 1110 Shimogato, Chuo 409-3898, Japan
Tel. +81-55-273-1111 (ext. 2382); Fax +81-55-273-6744
e-mail: masahori@yamanashi.ac.jp

H. Kabasawa
Department of Radiology, University of Tokyo, Tokyo, Japan

N. Shiraga
Department of Radiology, Toho University Omori Medical Center, Tokyo, Japan

M. Hori · S. Aoki
Department of Radiology, School of Medicine, Juntendo University, Tokyo, Japan

Introduction

High-spatial resolution susceptibility-weighted imaging (SWI) is an emerging magnetic resonance imaging (MRI) technique that provides complementary information on the venous vasculature, hemorrhage, and iron in the brain because it exploits both magnitude and phase shift to enhance susceptibility changes.[1–3] SWI also shows promise for evaluating brain tumors in clinical use to investigate their features by showing anatomical and functional heterogeneity.[4–7]

Some reports showing the usefulness of SWI in brain tumor evaluation have emphasized its ability to detect vasculature and microhemorrhages in brain tumors compared with conventional MRI techniques.[6,7] However, the contrast of brain tumors with SWI is not simply T2*-weighted imaging and remains to be clarified, using contrast material (gadolinium chelates) in particular. After administration of contrast medium, the T1- and T2-shorthening effect may influence the image contrast on SWI, and it is difficult to assume the contrast of within and around brain tumors. In a past report,[4] the

image quality of slow-flow vessels on SW images was improved by using a T1-reducing contrast material. Theoretically, intratumoral vasculature may be clearly visualized as low signal structures on SWI. However, both the solid tumor component enhanced by interstitial leakage of contrast medium due to breakdown of the blood-brain barrier (BBB) and a pool of contrast medium in the tumor's neovasculature showed an enhancement effect (higher signal area) on contrast-enhanced SWI.[4,5] Moreover, some data-processing steps are needed to create the final SW images (i.e., using high pass filtered phase images and multiplying the mask several times with the higher magnitude images). Therefore, the contrast changes are based not only on T1 or T2 values but also on processes of image reconstruction. Clinically, it is expected that brain tumors with different pathologies, intraaxial and extraaxial brain tumors in particular, may show different signal patterns because the breakdown of the BBB often accompanies intraaxial brain tumors.

The purpose of this study was to estimate the pre- and post-contrast-enhanced SWI in patients with brain tumors for clinical use.

Materials and methods

Patients

A total of 17 patients (8 women, 9 men) with brain tumors participated in this study. Among these 17 patients, clinical diagnoses were glioblastoma ($n = 5$), anaplastic astrocytoma ($n = 4$), low-grade astrocytoma ($n = 1$), metastatic tumor ($n = 2$), central nervous system (CNS) lymphoma ($n = 1$), meningioma ($n = 3$), and schwannoma ($n = 1$). In 13 of the 17 patients, the final pathology results were obtained from surgical specimens. Two metastatic brain tumors were diagnosed based on clinical information of systemic metastatic tumors and follow-up studies: One was a schwannoma diagnosed clinically recognizing that the patient had neurofibromatosis type II with no interval changes in the MRI findings; the second metastatic tumor was diagnosed as a low-grade astrocytoma by a series of MRI scans and spectroscopy.

Magnetic resonance imaging

All MRI studies were performed on a 1.5-T MRI instrument (Signa Excite HD, software version 12; GE Healthcare, Milwaukee, WI, USA) with an 8-channel phased array head coil. Imaging parameters of three-dimensional (3D) SWI were as follows: repetition time/echo time (TR/TE) 53/40 ms; matrix 384 × 256; bandwidth 15.6 kHz; field of view (FOV) 240 × 180 mm; partition thickness/gap 1.5/0 mm; number of partitions 28 mm; flip angle (FA) 30°; number of average 1; total scan time 5 min 29 s. Moreover, the imaging parameters for 3D T1-weighted gradient-echo imaging, for direct comparison imaging, were as follows: TR/TE 28/ 3 ms; matrix 256 × 192; bandwidth 15.6 kHz; FOV 220 × 220 mm; partition thickness/gap 1.4/0 mm; number of partitions 32; FA 30°; number of average 1; total scan time 3 min 17 s. The MRI protocol consisted of conventional MRI sequences, pre- and post-gadolinium-enhanced SWI, and post-gadolinium-enhanced 3D T1-weighetd gradient-echo imaging. Conventional MR examinations consisted of fast spin-echo (FSE) T2-weighted imaging (TR/TE/echo train length 3100 ms/83 ms/14); spin-echo T1-weighted imaging (TR/TE 420/9 ms); FSE fluid-attenuated inversion recovery (FLAIR) imaging (TR/TE/inversion time 9000/107/2250 ms); and gradient echo T2*-weighted imaging (TR/TE/flip angle 520 ms/20 ms/20°).

Image analysis

All SW images were evaluated visually by two neuroradiologists, who compared them with conventional sequences and postcontrast 3D T1-weighted images on a slice-by-slice basis. For quantitative analysis, the maximum diameter of the brain tumor was measured on postcontrast SWI and 3D T1-weighted images.

For another quantitative analysis, the contrast-to-noise ratio (CNR) was measured and compared between the enhanced pathological lesions and normal brain

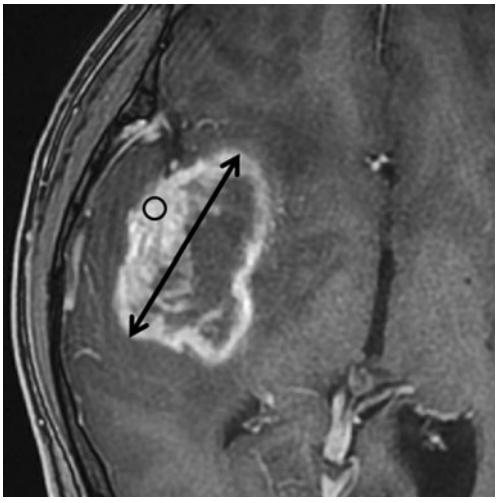

Fig. 1. Typical example of a measurement of the maximum tumor diameter (*line with arrows*) and region of interest (ROI) on the enhanced lesion (*circle*) on a contrast-enhanced T1-weighted image

white matter on postcontrast SW images and 3D T1-weighted images. The CNR was calculated using the following formula.

$$[SI_{tumor} - SI_{white\ matter}]/SD_{background}$$

where SI_{tumor} is the mean signal intensity in the region of interest (ROI) in the clearly enhanced area of the tumors; $SI_{white\ matter}$ is the surrounding normal-appearing white matter; and $SD_{background}$ is the standard deviation of the background noise in the frequency-encoding direction.

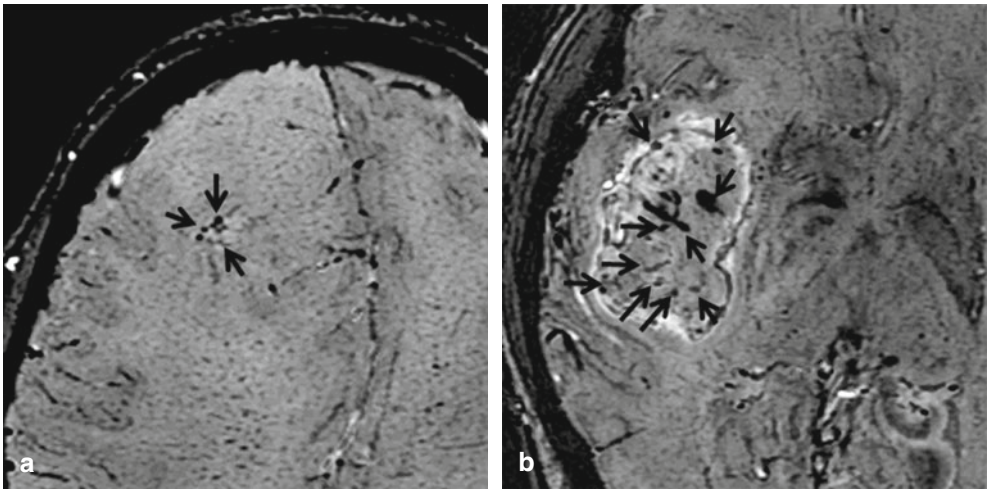

Fig. 2. Typical images of the intratumoral susceptibility signal intensity (ITSS). **a** Grade 2 ITSS indicates 6–10 dot-like or linear low-intensity structures (*arrows*) in a case of anaplastic astrocytoma. **b** Grade 3 ITSS indicates ≥ 11 ITSSs in the continuous area (*arrows*) within a glioblastoma

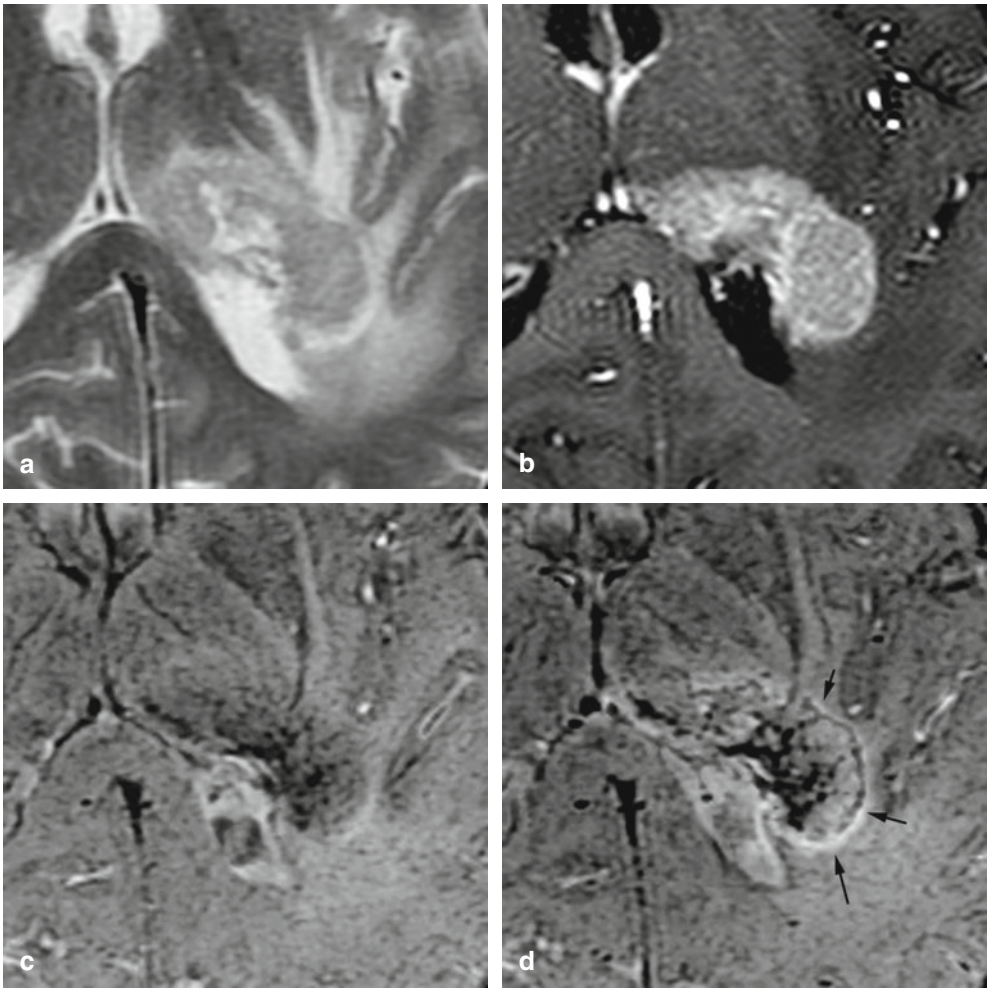

Fig. 3. Malignant lymphoma in a 54-year-old man. **a** Axial T2-weighted image shows a mass lesion along the left lateral ventricle. **b** Contrast-enhanced axial T1-weighted image shows tumor heterogeneity. **c** Non-contrast-enhanced axial susceptibility-weighted imaging (SWI) shows much more vasculature and blood products in the tumor than does contrast-enhanced T1-weighted imaging. **d** Contrast-enhanced axial SWI shows more clearly the internal structure than noncontrast SWI. Bright enhancement (*arrows*) indicating breakdown of the blood-brain barrier is seen along the tumor rim

One ROI including at least 10 pixels was placed on each postcontrast SW image and 3D T1-weighted image for every patient (Fig. 1).

For the semiquantitative analysis, we graded the degree of intratumoral susceptibility signal intensity (ITSS) on pre- and post-contrast-enhanced SWI scans.[8] With this evaluation, the degree of ITSS was assigned a grade from 0 to 3: grade 0, no ITSS; grade 1, one to five dot-like or linear ITSSs; grade 2, six to ten ITSSs; and grade 3, eleven or more ITSSs in the continuous area within a tumor (Fig. 2).

Results

Both bright and dark enhancement, which were showed as enhanced areas on contrast-enhanced T1-weighted images, were observed at the pathological lesion on post-contrast SW images. Postcontrast SW images showed bright enhancement (Figs. 3, 4) along the tumor that suggested leakage of contrast material due to breakdown of the blood-brain barrier only on the nine intraaxial malignant tumors. Precontrast SW images showed the edema surrounding tumors to the same extent compared with T2-weighted and FLAIR images (Fig. 5); they also revealed blood products more clearly than T2*-weighted images. The major diameters of the brain tumors had no statistically differences (Student's *t*-test) between post-contrast SW images and 3D T1-weighted images. However, an abnormally enhanced diameter was wider in the postcontrast SW images in all 17 cases.

The CNR of postcontrast 3D T1-weighted images and postcontrast SW images were 50.4 ± 15.5 and 17.9 ± 9.20, respectively (values represent the mean ± SD). The CNR of postcontrast 3D T1-weighted images was statistically superior to that of postcontrast SW images ($P < 0.01$, Wilcoxon signed-rank test).

The results of the semiquantitative analysis indicated that the grading scores for high-grade astrocytic tumors (including glioblastoma and anaplastic astrocytoma) were 2.6 ± 0.8 on pre-SWI and 2.7 ± 0.5 on post-SWI (values represent mean ± SD). The score for the low-

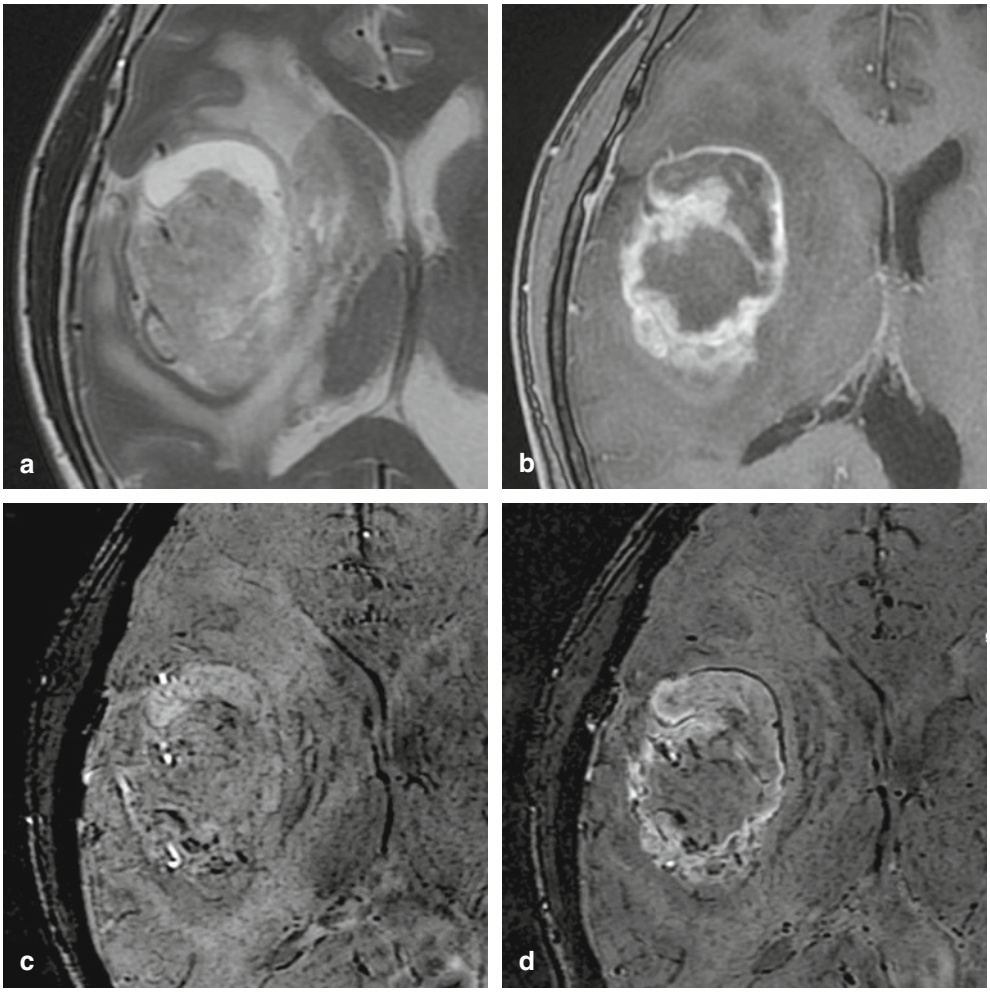

Fig. 4. Glioblastoma in a 58-year-old man. **a** Axial T2-weighted image shows a heterogeneous mass lesion with edema. **b** Contrast-enhanced axial T1-weighted image shows intratumoral heterogeneity. **c** Non-contrast-enhanced axial SWI shows significantly more vasculature and blood products in the tumor, but the border is not clearly identified compared with that seen with contrast-enhanced T1-weighted imaging. **d** Contrast-enhanced axial SWI shows the internal structure more clearly than noncontrast SWI. Moreover, bright enhancement indicating both tumor parenchyma and breakdown of the blood-brain barrier are seen in and along the tumor, respectively

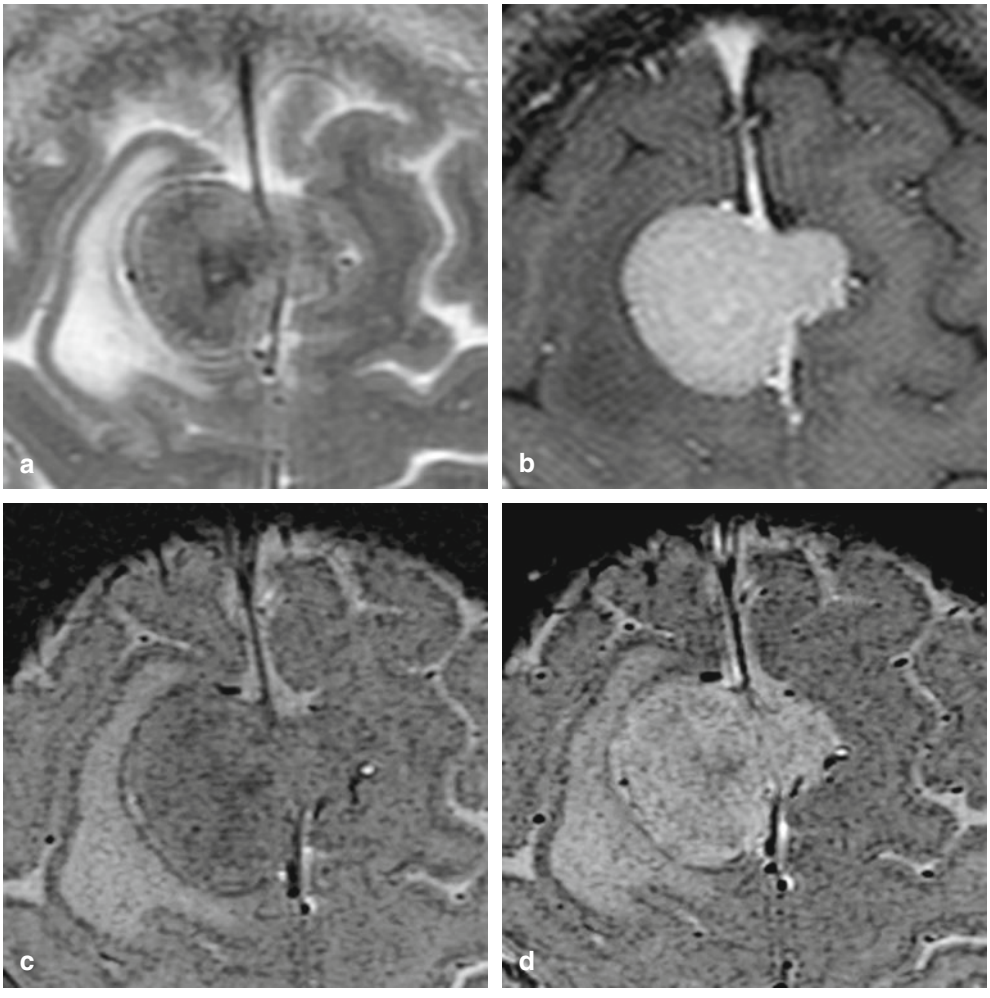

Fig. 5. Meningioma in a 56-year-old woman. **a** Axial T2-weighted image shows a mass lesion with edema. **b** Contrast-enhanced axial T1-weighted image shows tumor enhancement. **c** Non-contrast-enhanced axial SWI shows tumor with edema to the same extent as with T2-weighted imaging. **d** Contrast-enhanced axial SWI shows tumor enhancement similar to that seen with contrast-enhanced T1-weighted imaging. Note that no bright enhancement is seen surrounding the tumor

grade astrocytoma was 0. Malignant tumors (including metastatic brain tumors and CNS lymphoma) were all scored 3 on both pre- and post-SWI. Schwannoma and meningiomas showed various scores, from 1 to 3.

Discussion

The SWI technique clearly visualized the characteristics and architecture of brain neoplasms.[4–8] This imaging technique provides more information in addition to conventional sequences and is useful for evaluating brain tumors in vivo, particularly with contrast enhancement. However, our results showed that the CNR of post-contrast-enhanced images were inferior on SWI. This is natural because SWI is the sequence based on 3D T2*-weighted imaging. Therefore, we guess that SWI is a preferable sequence to investigate known neoplasms in the brain but is not preferable for *detecting* lesions (i.e., screening for brain metastasis in patients with a malignant lesion outside the brain). In fact, unlike other MRI sequences, both enhancement and signal cancelation may be seen on postcontrast SWI, depending on the condition of the pathological lesion. Moreover, our results showed that measurement of tumors using post-contrast SWI was not problematical. Therefore, this technique has the potential to replace some conventional sequences in routine clinical studies.

As described in the literature,[6,8] our results also showed that malignant tumors tended to be scored with a higher value. It is natural that the vasculature and microhemorrhages in brain tumors may be more frequently visualized, particularly in astrocytic tumors. Park et al. reported that SWI on 3-T MRI is useful for grading gliomas, but they think that SWI on 1.5-T MRI is time-consuming for routine MRI.[8] However, we think that SWI on 1.5-T MRI for evaluating potential malignant brain neoplasms should be available for clinical use because the intratumoral vasculature is more clearly visualized[9] and there is improved contrast between the ITSS and background when the solid part of the tumor is enhanced with the use of contrast material. As con-

cerns meningiomas and schwannomas, ITSS on SWI may correlate only the vasculature or necrosis. Therefore, we guess that SWI is less useful for benign brain neoplasms than for tumors with malignant potential.

Limitations of our study are the small number of patients and their heterogeneous pathologies. More patients must be studied to establish the clinical usefulness of SWI.

Another potential limitation is our method for evaluating SWI in this study. We measured the diameters of lesions and CNRs, as described above, and estimated the susceptibility effect in the method for grading ITSS.[8] It was difficult to estimate the effects quantitatively because they were easily changed by the parameters, such as the echo time and postprocessing filters. Therefore, several methods of evaluation should be introduced to establish the usefulness of SWI in any future studies.

Conclusion

The combination of precontrast and postcontrast SWI scanning provides adjunct information for evaluating the structural characteristics of brain tumors. In clinical use it is also useful for differentiating malignant from benign tumors even with 1.5-T MRI.

References

1. Haacke EM, Xu Y, Cheng YC, Reichenbach JR. Susceptibility weighted imaging (SWI). Magn Reson Med 2004;52:612–8.
2. Rauscher A, Sedlacik J, Barth M, Haacke EM, Reichenbach JR. Noninvasive assessment of vascular architecture and function during modulated blood oxygenation using susceptibility weighted magnetic resonance imaging. Magn Reson Med 2005;54:87–95.
3. Rauscher A, Sedlacik J, Barth M, Mentzel HJ, Reichenbach JR. Magnetic susceptibility-weighted MR phase imaging of the human brain. AJNR Am J Neuroradiol 2005;26:736–42.
4. Sehgal V, Delproposto Z, Haacke EM, Tong KA, Wycliffe N, Kido DK, et al. Clinical applications of neuroimaging with susceptibility-weighted imaging. J Magn Reson Imaging 2005; 22:439–50.
5. Sehgal V, Delproposto Z, Haddar D, Haacke EM, Sloan AE, Zamorano LJ, et al. Susceptibility-weighted imaging to visualize blood products and improve tumor contrast in the study of brain masses. J Magn Reson Imaging 2006;24:41–51.
6. Pinker K, Noebauer-Huhmann IM, Stavrou I, Hoeftberger R, Szomolanyi P, Karanikas G, et al. High-resolution contrast-enhanced, susceptibility-weighted MR imaging at 3T in patients with brain tumors: correlation with positron-emission tomography and histopathologic findings. AJNR Am J Neuroradiol 2007;2:1280–6.
7. Pinker K, Noebauer-Huhmann IM, Stavrou I, Hoeftberger R, Szomolanyi P, Karanikas G, et al. High-field, high-resolution, susceptibility-weighted magnetic resonance imaging: improved image quality by addition of contrast agent and higher field strength in patients with brain tumors. Neuroradiology 2008;50:9–16.
8. Park MJ, Kim HS, Jahng GH, Ryu CW, Park SM, Kim SY. Semiquantitative assessment of intratumoral susceptibility signals using non-contrast-enhanced high-field high-resolution susceptibility-weighted imaging in patients with gliomas: comparison with MR perfusion imaging. AJNR Am J Neuroradiol 2009;30:1402–8.
9. Lin W, Mukherjee P, An H, Yu Y, Wang Y, Vo K, et al. Improving high-resolution MR bold venographic imaging using a T1 reducing contrast agent. J Magn Reson Imaging 1999;10:118–23.